

PHYSICS INVESTIGATION

Selective and super-selective C-arm based cone beam CT angiography (CBCTA) with DynaCT for CyberKnife radiosurgery planning of intracranial arteriovenous malformations (AVMs)

Oliver Edwin Holmes, MD, MSc, FRCPC^{1,2,3}, Janos Szanto, PhD, FCCPM⁴, Vered Tsehmaister Abitbul, MD⁵, Taleb Al Mansoori, MBBS, DABR, FRCPC⁶, Hanan Al-Qahtani, MD⁵, John Sinclair, MD, FRCSC, BSc⁷, Daniela Iancu, MD, MSc⁵ and Shawn Malone, MD, FRCPC³

¹Division of Radiation Oncology, Dr. H. Bliss Murphy Cancer Centre, St. John's, NL, Canada

²Faculty of Medicine, Memorial University of Newfoundland, St. John's, NL, Canada

³Division of Radiation Oncology, University of Ottawa, Ottawa, ON, Canada

⁴Department of Medical Physics, Ottawa Hospital Cancer Centre, Ottawa, ON, Canada

⁵Department of Radiology, University of Ottawa, Ottawa, ON, Canada

⁶Radiology Department, College of Medicine and Health Sciences, Al Ain, United Arab Emirates

⁷Department of Neurosurgery, University of Ottawa, Ottawa, ON, Canada

Correspondence to: Oliver Edwin Holmes, MD, MSc, FRCPC, Division of Radiation Oncology, Dr. H. Bliss Murphy Cancer Centre, 300 Prince Phillip Drive, St. John's, NL, Canada, K1H 8L6; Email: oliver.holmes@easternhealth.ca; Phone: +1 (709) 777-2440; Fax: +1 (709) 777-8756

(Received: March 1, 2018; Accepted: June 13, 2018)

ABSTRACT

Background: Successful radiosurgery for intracranial arteriovenous malformations (AVMs) requires accurate delineation of the nidus in 3D. Exact targeting and precise equipment is needed to achieve obliteration of the nidus while minimizing toxicity to the surrounding brain. In some micro-AVMs and poorly visible AVMs we have used cone beam CT angiography (CBCTA) with selective and super-selective angiography -where a micro-catheter is advanced into the feeding arteries- to assist with nidus definition for CyberKnife radiosurgery planning.

Methods: Four patients who had AVMs inadequately visualized with MRI, MRA, CT, CTA, and dynamic CT angiography (dCTA) were identified for selective angiography (2 had super-selective angiography) for CyberKnife radiosurgery. The mean age at the time of treatment was 45 years (range: 22 – 71 years). All patients had suffered prior hemorrhage and were deemed inoperable. Super-selective angiography was done under general anesthesia to minimize motion artefact and the risk of arterial dissection. Angiography was performed using the biplane angiographic suite (ArtisQ; Siemens). Cone beam reconstructions were performed using DynaCT software. For each scan, volumetric data was acquired over 20 seconds in a single rotation of the C-arm mounted flat-panel detector cone-beam CT system. The data set was imported into the CyberKnife TPS and co-registered with the treatment planning CT, T2 MRI and Toshiba dCTA. Delineation of the AVM nidus was performed by the multi-disciplinary AVM team.

Results: There were no adverse events related to the angiography or radiosurgery treatment. CBCTA data sets created using DynaCT were accurately co-registered with the treatment planning scans in

the CyberKnife treatment planning system (Multiplan). For all 4 patients, feeding arteries, draining veins and nidi were clearly visualized and used to develop radiosurgery plans. Mean nidus size was 0.45cc (range: 0.07 – 1.00cc).

Conclusions: For intracranial micro-AVMs and AVMs otherwise poorly visualized using DSA, MRA, CTA or dCTA, selective and super-selective CBCTA images (created using DynaCT) can be successfully imported into the CyberKnife TPS to assist in nidus delineation. Advancement of a micro-catheter into the feeding arteries to allow continuous contrast injection during volumetric scanning constitutes super-selective CBCTA. This technique provides superior visualization of micro-AVMs and should be utilized for radiosurgery planning of poorly visualized AVMs.

Keywords: radiosurgery, arteriovenous malformations, C-arm based cone beam CT angiography (CBCT-A), CyberKnife radiosurgery, selective angiography, intracranial arteriovenous malformation

INTRODUCTION

Intracranial arteriovenous malformations (AVMs) are rare vascular anomalies present in 0.01-0.05% of the population (1). They are tortuous network of vessels shunting blood flow directly from the arterial supply to the venous drainage bypassing the capillary bed. Without the resistance of a capillary bed there is higher than normal flow which causes the nidus and draining veins to grow over time. The disorganized tangle of vessels is prone to bleeding. Intracranial AVMs have a 1-5% annual risk of hemorrhage (2-3). The lifetime risk of hemorrhage is clinically significant, as patients are typically diagnosed between the ages of 20 and 40, and there is high associated morbidity (53-81%) and mortality (10-17.6%) (1-4).

Treatment options are aimed at reducing the risk of hemorrhage and generally include surgical resection, endovascular embolization and radiosurgery. Microvascular surgery is the treatment of choice in most cases. However, radiosurgery (RS) is preferred when the operative risk is high: in small deep-seated AVMs, those in eloquent areas of the brain, and in medically inoperable patients. RS can also be useful as part of multi-modality approach in larger AVMs (5). Radiosurgery is an excellent option for intracranial AVMs, with 3 year obliteration rates of 60-80% (1,4,5).

The underlying radiobiologic mechanism behind radiosurgery for AVM's is the induction of late tissue effects in the nidus by using high dose per fraction radiotherapy. Long after radiosurgery, endothelial hyperplasia (a known late effect of radiotherapy) is thought to cause gradual narrowing and eventual occlusion of the feeder vessels, and obliteration of the nidus (6). Precise equipment and targeting is needed to achieve obliteration of the nidus while minimizing toxicity to the surrounding brain. Targeting error is an important mode of treatment failure and subsequent need for retreatment (7-9).

High resolution catheter biplane digital subtraction angiography (DSA) remains the gold standard for differentiating the nidus from feeding arteries and veins (due to superior spatial and temporal resolution). But, DSA images are 2D in nature and are of limited use in 3D RS planning. Furthermore, DSA images are frame based and cannot be accurately co-registered in the CyberKnife (CK) treatment planning system (TPS). During treatment, the CyberKnife system uses two orthogonal KV X-ray units mounted in the ceiling to obtain simultaneous mutually perpendicular images of the skull. KV images are automatically compared to digitally reconstructed radiographs (DRRs) which represent the position of the skull during the planning scan. The skull tracking algorithm matches the real time images to the DRRs thereby calculating the physical position of the lesion in real time in the treatment frame. The CyberKnife robotic arm automatically adjusts to target motion and misalignment during the treatment. This strategy avoids the use of an invasive head frame, and allows elective RS planning and treatment.

In the CyberKnife TPS the AVM volume is defined using multiple 3D imaging modalities: CT angiograms (CTA), dynamic CT angiography (dCTA) and MR angiograms (MRA). These 3D image sets are coregistered to the planning CT scan using the patient's bony anatomy. While CTA and MRA provide excellent 3D localization of the vascular tree, they are static in nature and unlikely to represent the optimal time-point where contrast highlights the nidus. Previously, we described the integration of unsubtracted dCTA angiograms from a Toshiba CT scanner for AVM CK RS (12). While this technique represented a significant improvement over existing methods, accurate delineation of the nidus can still be a challenge. In select small AVMs the nidus is only visible on DSA owing to its high spatial resolution (13).

Typically DSA images are created using a C-arm fluoroscopy system in an angiography suite. Many C-arm systems are capable of performing 3D rotational angiography (3DRA). A filtered back projection algorithm can

be applied to create tomographic data: cone beam CT (CBCT). Selective angiography with 3D DynaCT digital angiography (DynaCTA) provides excellent spatial resolution for identification of small intracranial vascular lesions – including AVMs (13-16). DynaCTA datasets (which are CBCT's) have been used for frameless stereotactic intra-operative navigation, for Gamma Knife (GK) and CyberKnife (CS) radiosurgery of cerebrovascular lesions (16,17,18). In these studies, standard 4 vessel angiography (selective angiography) was done under local anesthesia. There was no advancement of a microcatheter beyond the skull base to the AVM feeding arteries (super-selective angiography). To our knowledge there are no existing reports describing the use of super-selective angiography with DynaCTA reconstruction for radiosurgery.

MATERIALS AND METHODS

At our institution, we routinely perform 6 vessel catheter angiography to investigate AVMs and dural AV fistulae. Within the paired vertebral, internal and external carotid arteries a catheter is sequentially advanced to the skull base to release contrast dye while digital images are acquired. In patients with micro-AVMs, a microcatheter can be advanced further into the feeding arteries to allow more direct enhancement and superior visualization of the AVM (*super selective* angiography). Using DynaCTA we have created 3D super selective CBCTA images of micro-AVMs and used those 3D data sets for CyberKnife radiosurgery planning.

Angiography Technique

Patients are under conscious sedation for standard 6 vessel angiography. General anesthesia is considered for patients with low GCS or when a super selective scan is planned, to minimize motion artefact and the risk of procedure induced arterial dissection. An 11 cm 5F Prelude Pro Introducer sheath (Mart Medical, South Jordan, Utah, USA) is introduced into the femoral artery and attached to a constant 0.9% Normal Saline drip. Selective catheterization of both internal carotid arteries, external carotid arteries and vertebral arteries is performed using 100 cm 5F VER diagnostic catheter (Cordis Corporation, Miami Lakes, Florida, USA) over 0.035" Glidewire (Terumo Medical Corporation, New Jersey, USA). *Super selective* catheterization of the feeding artery is performed using Excelsior SL-10 microcatheter (Stryker, Fremont, California, USA) over 0.0140" Traxcess 14 guidewire (Microvention, Tustin, California, USA) after navigating through 6F ENVOY XB guiding catheter (Codman, Raynham, Massachusetts, USA). 20 mL

of iodinated contrast media ISOVUE Multipack 300 (Bracco Imaging, Montreal, Quebec, Canada) diluted in 80 mL of normal saline are injected through the diagnostic catheter into the feeding artery using a double piston power injector (Medrad, Indianola, Philadelphia, USA).

Imaging and Co-Registration

We use the ArtisQ biplane digital angiography system (Siemens Medical Solutions, Forchheim, Germany). Volumetric data is acquired with a single rotation of the C-arm mounted flat-panel detector cone-beam CT system and reconstructed using DynaCT. If awake, patients are asked to hold their breath during the exam. The device parameters for are as follows: Tube voltage 70 kV, scan time 20 seconds, detector size 30 × 40 cm, effective detector resolution 960 × 1,240 pixels, maximum rotation angle 240°, 0.4° increments, total frames 543, dose 1.2 µGy/frame.

Post processing of the volumetric data is done using Syngo 4D software workstation (Siemens, Forchheim, Germany). Scatter and beam hardening artefacts are algorithmically minimized. The result is 3D dataset consisting of 400-550 512×512 slices spacing representing the patients entire head. Slice thickness 0.2mm, slice separation 0.5mm, voxel size 0.2x0.2x0.2mm.

The non-subtracted data set is imported into the CyberKnife TPS (MultiPlan version 4.6.0) and co-registered with the treatment planning CT, T2 MRI and Toshiba dCTA using the skull itself for alignment. Delineation of the AVM nidus was performed by the multi-disciplinary AVM team.

Patient Population

Between, 2016 and 2017, 4 Patients who had AVMs inadequately visualized with MRI, MRA, CT, CTA, including dCTA were identified for selective angiography (2 had super-selective angiography). The mean age at the time of treatment was 45 years (range: 22 – 71 years). All patients had suffered prior hemorrhage and were deemed inoperable. Selective DSA angiograms are routinely performed for diagnostic evaluation of vascular lesions at our institution. In these four cases, Intra Arterial DynaCTA was acquired and coregistered in the treatment planning system for radiosurgery.

RESULTS

Case 1

A 70 year old man woke up with a severe headache. A non-contrast CT scan performed in the emergency

room showed a left cerebellopontine angle hemorrhage. Initially, no vascular abnormality or cause of bleeding was demonstrated on MRI and cerebral angiography. A follow up angiogram 7 months later showed evidence of a small (2-3mm) AVM in the left posterior fossa fed by a small branch of the superior cerebellar artery. The nidus was not visualized well enough with cerebral angiography for CyberKnife RS planning. Super-selective DynaCTA was performed with the patient under general anesthesia demonstrating a tiny 74mm³ AVM. Unsubtracted angiography images were imported into the CK TPS for target delineation. The patient was treated with 18Gy in a single fraction to the 85% isodose.

Case 2

21 year old woman with a history of congenital deafness was found unresponsive and incontinent of stool. She was taken to the local hospital where a non-contrast CT scan of the brain showed that she had sustained a left basal ganglia hemorrhage (see Figure 2). Subsequent imaging showed an AVM in the left basal ganglia. Considering the eloquent location of her AVM,

the multidisciplinary team favoured radiosurgery treatment. CTA, MRA, dCTA and DynaCT images were coregistered in the treatment planning system for the targeting purposes. There was a significant discrepancy in the location of the nidus due to the slowly resolving hemorrhage. The hemorrhage had caused a mass effect and edema and it was challenging to properly define the limits of the AVM. CBCTA DynaCTA and dCTA were repeated 3 months later. The CT datasets were again coregistered in the treatment planning system. This time there was excellent agreement in the location of the nidus. Her 3.0cm³ AVM was treated on CyberKnife with a single 16.5 Gy fraction prescribed to the 78% isodose.

Case 3

A 22 year old pregnant woman developed a sudden headache and collapsed. A CT scan in the emergency room showed a massive intraventricular and intracerebral hemorrhage secondary to an AVM of the septum pellucidum. She was transferred to the ICU in a coma. She had a large intraventricular clot complicated by

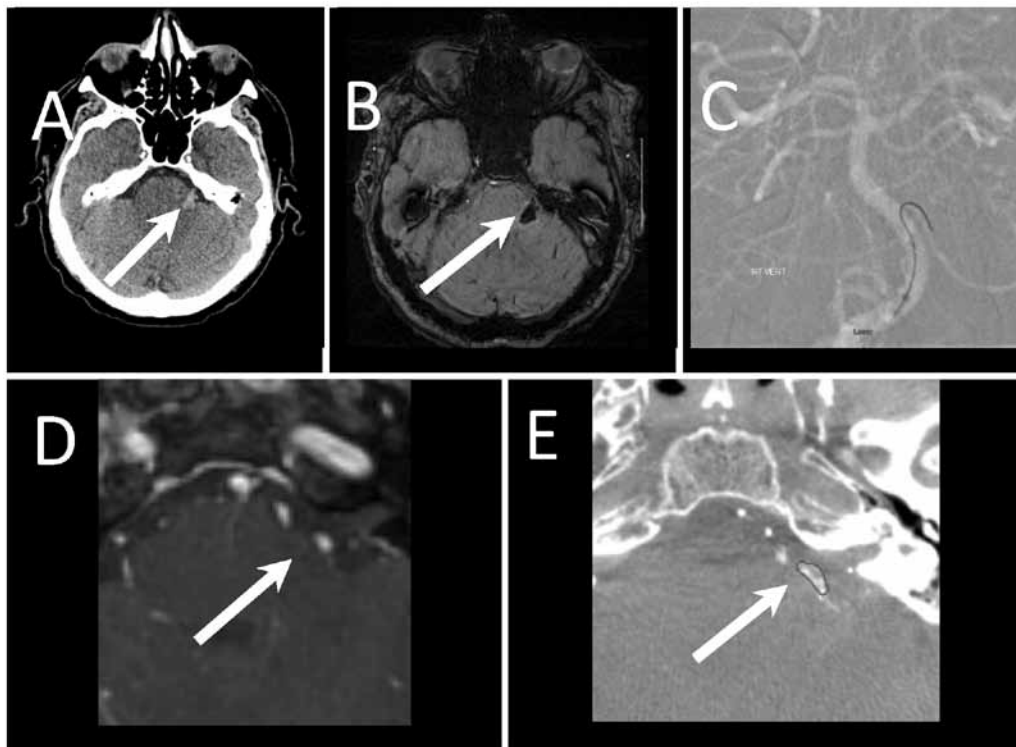


Figure 1. (A) Axial slice from initial non-contrast enhanced CT scan showing L CP angle hemorrhage. (B) Initial MR imaging (Axial susceptibility weighted MRI images) showed hemorrhage but no vascular lesion. (C) Fluoroscopy image demonstrating the advancement of a catheter into the left cerebellar artery. (D) MRA image fails to clearly demonstrate location of the nidus. (E) DynaCT coregistered in the planning system with the nidus contoured. The intra-arterial catheter is seen as an area of high density within the left cerebellar artery (arrow).

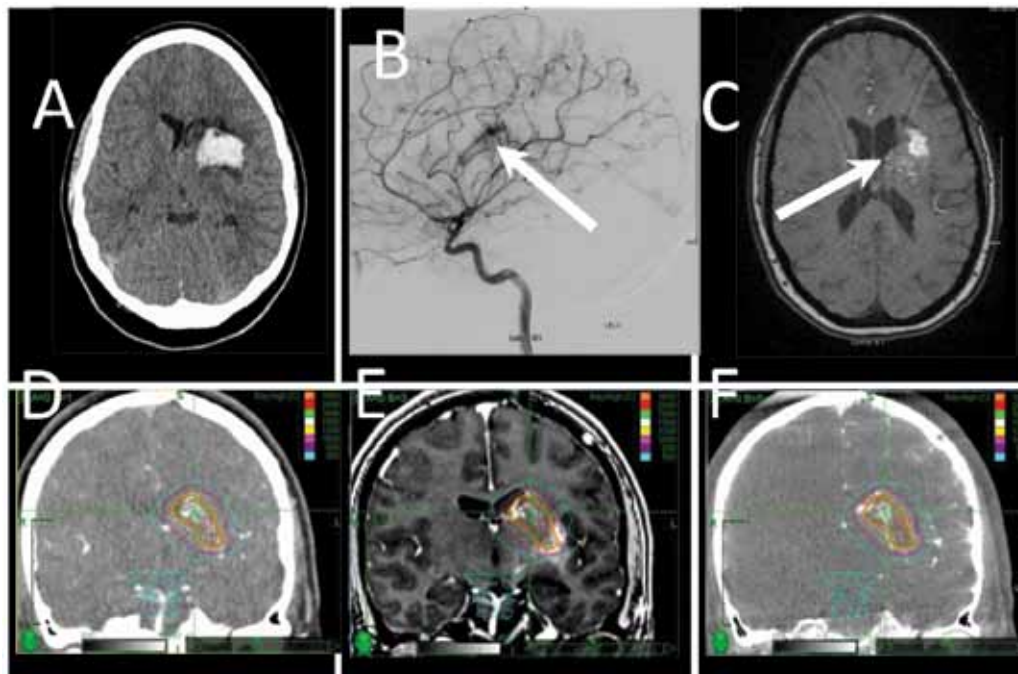


Figure 2. (A) Unenhanced emergency room CT showing a left basal ganglia hemorrhage. (B) DSA image showing 15mm nidus. (C) 3D TOF MRI sequence showing both the resolving hemorrhage and adjacent AVM nidus. (D) Coronal dynamic CT angiography image co-registered in CyberKnife Multiplan with the MRA (E) and DynaCTA (F) images.

obstructive hydrocephalus which was treated with a combination of ventricular drainage, tPA injection and ventriculoperitoneal (VP) shunt. 3 months later she underwent a bicoronal craniotomy under stereotactic guidance for a resection of the AVM. The bulk of the lesion was in the corpus callosum, but it extended to the septum pellucidum. There was a 1.5cm residual nidus adjacent to the vein of Galen that was felt to be too high risk for further resection. Two months later she had made an some neurologic recovery, but had a spastic gait and difficulties with short term memory. The residual AVM was treated with single fraction CyberKnife RS (15Gy) prescribed to the 80% isodose. RS Dose was limited by proximity of the nidus to the pineal region and mid brain. Follow-up angiographic imaging demonstrated gradual regression of her nidus, but after 4 years there was still residual arteriovenous shunting. She underwent selective angiography with an attempt at endovascular embolization with partial success.

6 years after her initial presentation her arteriovenous shunting persisted despite an additional attempt at transvenous embolization. Since further surgery was considered unsafe, and she had no further intravascular options she was treated with CyberKnife RS. Because of the complexity of the vascular supply selective angiography was repeated under general anesthesia, and the unsubtracted images were used for RS treatment planning.

Two separate nidus targets were identified with the super selective angiography; they were treated with single fraction RS 15Gy (60% isodose) and 20Gy (80% isodose).

Case 4

A 57 year old man was investigated in the emergency department for sudden onset aphasia and right sided weakness. A CT scan revealed a left posterior frontal hemorrhage. A catheter angiogram was performed to identify the source of bleeding. A small (423mm³) unrelated and unruptured AVM in the left posterior temporal lobe was found. The source of the hemorrhage (another AVM in the left frontal lobe) was not found until 4 months after the initial event on repeat DSA.

He underwent an awake craniotomy for resection of the previously ruptured left frontal AVM. The second AVM was later treated with radiosurgery (21Gy prescribed to the 78% isodose). Prior to radiosurgery a new time of flight MRA was performed, but the tiny left temporal AVM was not visualized. Repeat selective catheter angiography under local anesthesia redemonstrated the left temporal AVM. Unsubtracted DynaCT images were generated and imported into the RS planning system, along with the new MRA for targeting.

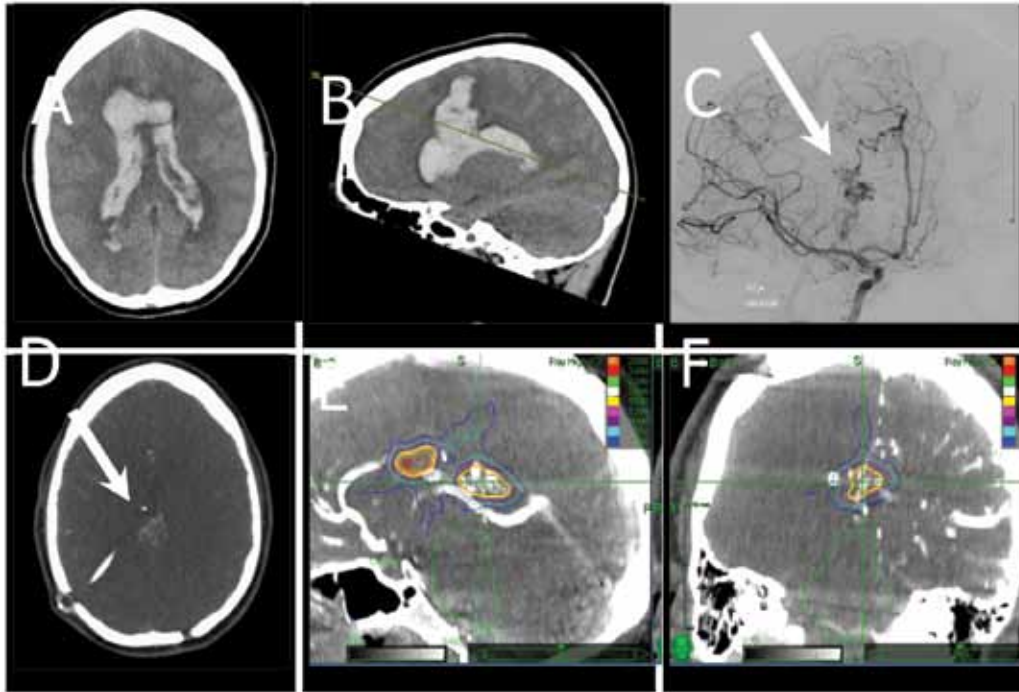


Figure 3. (A,B) Respectively, axial and sagittal unenhanced CT reconstructions from the emergency department showing a large intraventricular and parenchymal hemorrhage. (C) Catheter DSA image showing the large centrally located AVM. (D) Axial view of dCTA showing the residual AVM post resection. The VP shunt tube is also shown in this image. (E,F) Selective DynaCT angiogram which has been coregistered into the CK TPS for targeting, sagittal and coronal views are shown respectively. After multiple treatments the complex nidus is now 2 distinct lesions which were treated separately.

DISCUSSION

Successful radiosurgical treatment of an AVM nidus requires accurate delineation of the nidus in the treatment planning system. High dose per fraction radiation can then be tightly conformed to the target in order to minimize the risks of complications. It can be challenging to differentiate the target nidus from the complex architecture of feeding and draining vasculature. In addition there can be complex imaging changes on CT and MRI from prior hemorrhage. Inaccurate identification of the nidus can result in RS target errors causing treatment failure or late radiosurgery toxicity (7-9). Incomplete dose coverage of the AVM volume may yield only partial obliteration of the nidus. The risk of hemorrhage and survival in incompletely cured AVMs are similar to untreated AVMs (10). Similarly, the risk of radiation necrosis and other late complications from radiotherapy increases with higher volumes of healthy brain in the high dose region (11). Excellent imaging and careful target delineation are needed in order to achieve successful uncomplicated AVM radiosurgery.

A variety of imaging techniques are used in the diagnosis and characterization of AVMs. These techniques are also useful during RS planning. For example, CTA, MRA, dCTA, and DynaCTA can be imported directly into the RS planning system for increased targeting accuracy. DSA is the gold standard for visualizing AVMs, but despite superior temporal and spatial resolution it is of limited use in CK RS planning: 1) DSA images are 2D in nature and therefore cannot be used readily for 3D RS treatment. 2) DSA images are frame based and cannot be accurately coregistered in the CK planning system which relies on skull tracking. Conversely, CTA and MRA images are 3D in nature and are readily imported into the CyberKnife planning system for target definition. Nevertheless, they lack the temporal and spatial resolution needed to differentiate the AVM from its associated vasculature (12). In an effort to improve temporal resolution, our Radiosurgery team previously published on the use of dynamic (time resolved) CT angiography (dCTA) for radiosurgery. dCTA is a non-invasive vascular imaging technique that has been shown to provide both high temporal and spatial resolution in a 3D volume

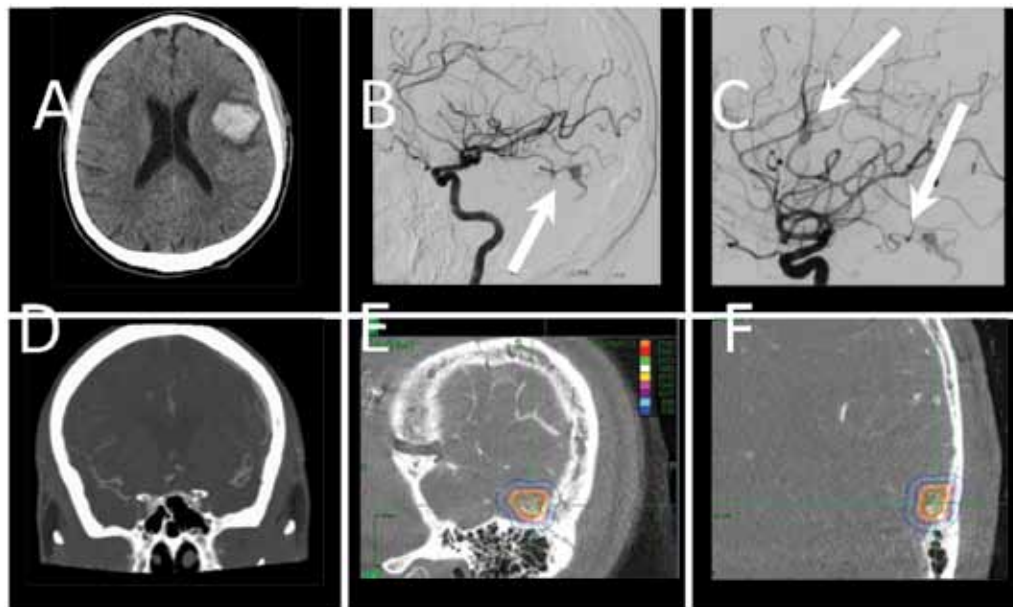


Figure 4. (A) This axial unenhanced CT reconstructed image performed in the emergency department for initial workup shows a left frontal hemorrhage. (B) Catheter DSA shows a microAVM in the left temporal lobe, which is unrelated to the hemorrhage, no vascular cause for the hemorrhage is seen. (C) Follow up catheter DSA again demonstrates the left temporal microAVM, but also identifies the cause of hemorrhage - a previously unseen left frontal microAVM. (D) Coronal image of dCTA showing early venous dilatation in the left opercular/perisylvian region. (E,F) Sagittal and coronal unsubtracted DynaCT images which have been imported into the CyberKnife planning system for targeting.

dataset. The entire cerebral volume can be imaged in a single rotation of the gantry, generating a full CT dataset of the cerebral vasculature every half second. The entire dataset represents 32 3D scans done over 16 seconds, representing time resolved brain images with temporal resolution of 0.5 sec. Typically, the single 3D set corresponding to the clearest image of the AVM is used for target delineation in the CyberKnife TPS (12). Some AVMs are poorly visualized using non-invasive techniques (13). In select AVMs it remains challenging to accurately define the extent of the nidus. This is particularly important when AVMs are located next to or in highly eloquent brain regions such as the brain stem, optic chiasm, thalamus and basal ganglia.

Invasive angiography typically involves advancement of a catheter originating from the femoral artery for direct injection of contrast into the vasculature of the brain. Fluoroscopic images can be acquired using a C-arm mounted flat-panel detector. Depending on the case, image processing and reconstruction are used to generate different types of images (DSA, 3D-RA, DynaCTA). Hiu et al presented a case series of 14 patients comparatively evaluat-

ing 2D DSA and DynaCT images in the detection of dural arteriovenous fistulas. Though their study was observational in nature, they reported that the isotropic spatial resolution was helpful in reliable visualization of the location of the fistulous points (15). Similarly, Namba et al used DynaCTA to clarify anatomical detail surrounding intracranial vascular lesions, detail which could not be seen either with DSA or conventional 3D-RA (14).

Improved anatomical detail allows localization of a lesion with respect to the surrounding anatomy, which is critical for any type of intervention (i.e., bones, vessels and eloquent tissue). Lim et al used 3D-RA and DynaCTA for precise localization of 3 dural arteriovenous fistulas. By correlating the 3D-RA and DynaCTA with CT images, the neurosurgeon could use neuronavigation in cases of AVF not appreciated on cross sectional imaging. Furthermore, the anatomical reference frame allowed accurate placement of fiducial markers and minimized the size of craniotomies needed to perform surgical intervention (13). DynaCT datasets have been used for neuronavigation in treatment for a variety of other cerebrovascular lesions inadequately imaged

Table 1. Patient characteristics

	Case 1	Case 2	Case 3	Case 4
Region	R cerebellopontine angle	L Basal Ganglia	Posterior pericallosal	L posterior temporal
Age	71	21	22	58
Sex	Male	Female	Female	Male
AVM Volume (cm ³)	0.07	3.0	1.2/1.3/0.31	0.42
AVM Diameter (cm)	~0.5	1.8	1.3/1.4/0.8	0.9
Dose (Gy)	18	16.5	15/15/20	21
Fractions	1	1	1	1
Rx Isodose (%)	85	78	80/60/80	78
Anesthesia	General	Local	General	Local
Angiography	Super-selective	Selective	Super-selective	Selective

or invisible to conventional pre-operative CTA and MRA and have been particularly helpful in surgical treatment of cerebral micro-AVMs (16).

A group from Tufts University recently reported on 22 AVM patients who received diagnostic catheter-based angiography (DSA, 3D-RA and DynaCTA) for GammaKnife radiosurgery. CBCT-A and 3-D RA imaging was performed with the Leksell stereotactic frame attached to the angiography table. In GK RS the frame itself is used to coregister images (such as CBCT-A images in this case) in the planning system. The CBCT-A and 3D-RA images provided excellent visualization of AVMs and associated vasculature for targeting (17). At a mean follow-up time of 16 months, they reported no nidus obliteration, but 56% had a decrease in nidus size.

By design, frameless robotic radiosurgery (i.e., CyberKnife radiosurgery) avoids the use of a stereotactic frame and allows angiography, targeting, and treatment to be done electively. The group at Stanford University, did a comparative analysis of CK treatment planning using conventional imaging with and without DynaCTA. They reported smaller AVM target volumes when DynaCTA was coregistered with MRA and CTA in the planning system compared to MRA or CTA alone. Whether the reduced target size translates to improved nidus obliteration or reduced toxicity requires more follow up data. As in our study, unsubtracted DynaCTA images allowed coregistration based on the bony anatomy of the skull (18).

While they are very similar in many respects, the Tufts and Stanford reports differ from the present study: The mean AVM volumes were substantially larger and there was no use of super selective angiography. We

provide a description of selective and super selective angiography with DynaCTA for CyberKnife radiosurgery planning for micro-AVMs and poorly visualized AVMs. We do not intend this report as a validation of super selective or selective angiography with DynaCTA for CK RS or recommend routinely using these techniques in place of DSA, CTA or MRA. We merely describe its use in cases where standard techniques are insufficient for RS treatment planning. Any observations made regarding patient outcomes in this small retrospective case series are affected by the usual biases of retrospective study and by limited patient numbers.

Geometric distortion of CBCT-A images is an important consideration when using DynaCTA for targeting microAVMs. In C-arm CBCT, spatial inaccuracy (up to 1.4mm) arises from “wobble” in the C-arm gantry (19). We acknowledge the importance of this potential source of error -particularly when treating sub-centimeter AVM’s- and we will characterize it in the context of radiosurgery planning in a separate report. In the present study, when AVM’s are well visualized there is excellent spatial agreement between image sets. Our follow-up time and patient numbers are insufficient to classify the long term success of these 4 microAVM’s treated with CK using CBCT-A and super selective or selective angiography for RS target delineation.

CONCLUSION

DSA remains the gold standard for imaging cerebrovascular AVMs. 2D DSA images should be used during the radiosurgery planning for AVMs, but they unfortu-

nately cannot be used for target delineation within the 3D treatment planning system. For intracranial micro-AVMs and AVMs otherwise poorly visualized using DSA, MRA, CTA or dCTA, selective and super-selective DynaCTAs can be successfully imported into the CyberKnife TPS to assist in nidus delineation. Super-selective angiograms are performed under the continuous administration of intra-arterial contrast in a steady state (avoiding the need for strict temporal resolution). Super selective CBCT-A (eg DynaCTA) provides superior contrast of micro-AVM's and may become the gold standard for radiosurgery planning of these small vascular lesions.

ACKNOWLEDGMENTS

Authors' disclosure of potential conflicts of interest

The authors have nothing to disclose.

Author contributions

Conception and design: Daniela Iancu, Oliver Holmes, Janos Szanto, Shawn Malone, John Sinclair

Data collection: Janos Szanto, Daniela Iancu, Oliver Holmes, Vered Tsehmaster Abitbul. Taleb Al Mansoori, Hanan Alqahtani

Data analysis and interpretation: Oliver Holmes, Janos Szanto, Shawn Malone, John Sinclair, Daniela Iancu

Manuscript writing: Oliver Holmes, Shawn Malone, Hanan Alqahtani, Taleb Al Mansoori, Vered Tsehmaster Abitbul

Final approval of manuscript: Oliver Holmes, Shawn Malone, Janos Szanto, Daniela Iancu, John Sinclair, Vered Tsehmaster Abitbul, Taleb Al Mansoori, Hanan Alqahtani

REFERENCES

1. Fleetwood IG, Steinberg GK. Arteriovenous malformations. *Lancet* 2002;359:823-73.
2. Brown Jr RD, Weibers DO, Forbes GS. Unruptured intracranial aneurysms and arteriovenous malformations: frequency of intracranial hemorrhage and relationship of lesions. *J Neurosurg* 1990;73:859-63.
3. Ondra SL, Troupp H, George ED, Schwab K. The natural history of symptomatic arteriovenous malformations of the brain: a 24-year follow-up assessment. *J Neurosurg* 1990;73:387-91.
4. Flemming KD, Lanzino G. Management of unruptured intracranial aneurysms and cerebrovascular malformations. *Continuum (Minneapolis Minn)* 2017;23(1):181-210.
5. van Beijnum J, van der Worp HB, Buis DR, al-Shahi Salman R, Kappelle LJ, Rinkel GJE, et al. Treatment of brain arteriovenous malformations: A systematic review and meta-analysis. *JAMA* 2011;306(18):2011-19.
6. Chang SD, Shuster DL, Steinberg GK, Levy RP, Frankel K. Stereotactic radiosurgery of arteriovenous malformations: Pathologic changes in resected tissue. *Clin Neuropathol* 1997;16:111-16.
7. Ellis TL, Freidman WA, Bova FJ, Kubilis PS, Buatti JM. Analysis of treatment failure after radiosurgery for arteriovenous malformations. *J Neurosurg* 1998;89:104-10
8. Pollock BE, Flickinger JC, Lunsford LD, Maitz A, Kondziolka D. Factors associated with successful arteriovenous malformation radiosurgery. *Neurosurgery* 1998;42:1239-44; Discussion 44-7.
9. Pollock BE, Kondziolka D, Lunsford LD, Bissonette D, Flickinger JC. Repeat stereotactic radiosurgery of arteriovenous malformations: factors associated with incomplete obliteration. *Neurosurgery* 1996;38:318-24
10. Gallina P, Merienne L, Meder JF, Schlienger M, Lefkopoulos D, Merland JJ. Failure in radiosurgery treatment of cerebral arteriovenous malformations. *Neurosurgery* 1998;42(5):996-1002.
11. Yamamoto M, Hara M, Ide M, Ono Y, Jimbo M, Saito I. Radiation-related adverse effects observed on neuro-imaging several years after radiosurgery for cerebral arteriovenous malformations. *Surg Neurol* 1998;49:385-98.
12. Haridass A, MacLean J, Chakraborty S, Sinclair J, Szanto J, Iancu D, Malone S. Dynamic CT angiography for cyberknife radiosurgery planning of intracranial arteriovenous malformations: a technical/ feasibility report. *Radiol Oncol* 2015;49(2):192-9.
13. Lim SP, Lesiuk H, Sinclair J, Lum C. Preoperative or preembolization lesion targeting using rotational angiographic fiducial marking in the neuroendovascular suite, *J Neurosurg* 2011;114:140-5.
14. Namba K, Niimi Y, Song JK, Berenstein A. Use of Dyna-CT angiography in neuroendovascular decision-making a case report. *Interv Neuroradiol* 2009;15:67-72.
15. Hiu T, Kitagawa N, Morikawa M, Hayashi K, Horie N, Morofuji Y, et al. Efficacy of DynaCT digital angiography in the detection of the fistulous point of dural arteriovenous fistulas. *Am J Neuroradiol* 2009;30:487-91.
16. Tee JW, Dally M, Madan A, Hwang P. Surgical treatment of poorly visualized and complex cerebrovascular lesions using pre-operative angiographic data as angiographic DynaCT datasets for frameless stereotactic navigation. *Acta Neurochir* 2012;154:159-67.
17. Safain MG, Rahal JP, Raval A, Rivard MJ, Mignano ME, Wu JK, Malek AM. Use of cone-beam computed tomography angiography in planning for Gamma Knife radiosurgery for arteriovenous malformations: A case series and early report. *Neurosurgery* 2014;74(6):682-96.
18. Veeravagu A, Hansasuta A, Jiang B, Karim AS, Gibbs IC, Chang SD. Volumetric analysis of intracranial arteriovenous malformations contoured for CyberKnife radiosurgery with 3-dimensional rotational angiography vs computed tomography/magnetic resonance imaging. *Neurosurgery* 2013;73(2):262-70.
19. Bridcut RR, Winder RJ, Workman A, Flynn P. Assessment of distortion in a three-dimensional rotational angiography system. *Br J Radiol* 2002;75:266-70.